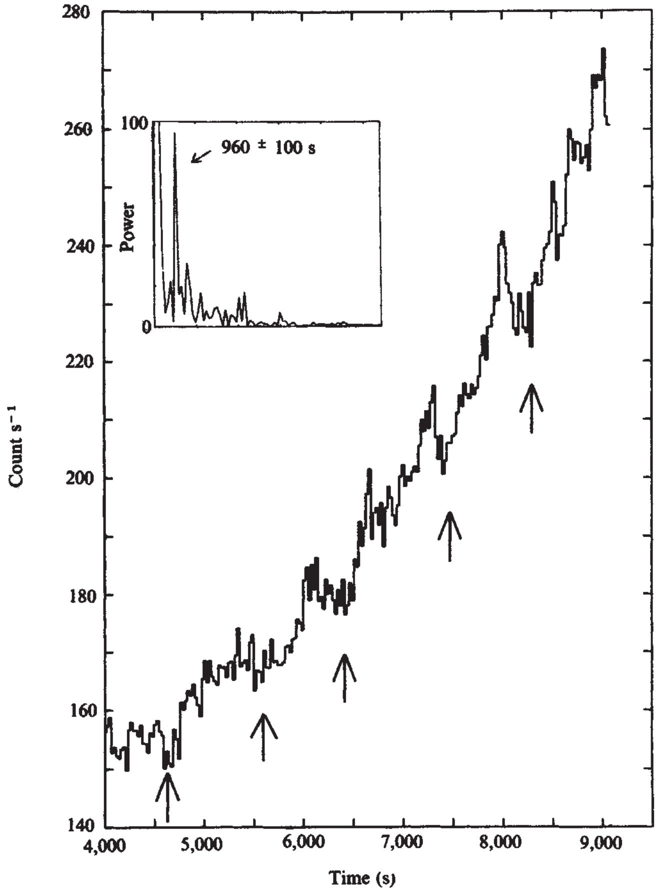

Fig. 3 As Fig. 2, but for the low state observed on 21 May 1984. Bin size is 24 s. The dips which contribute to the periodicity showing up in the power spectrum (inset) are indicated.

expansion, which would prevent a hypothetical red dwarf from overflowing its Roche lobe were it to follow approximately the mass-radius relation for low-mass main-sequence stars during its mass loss. Moreover, Cyg X-3 has very peculiar radio and possibly γ-ray emission properties. It is thus quite different from any of the low-mass X-ray binaries mentioned above, but the way in which their X-ray light curves are produced may well be similar.

M.v.d.K. thanks the Dutch Organisation for Pure Research ZWO (ASTRON) for financial support under contract 19-21-019 for part of this work.

Received 20 September; accepted 2 November 1984.

1. Dickey, J. M. *Astrophys. J.* **273**, L71–L73 (1983).
2. Gregory, P. C. *et al. Nature* **239**, 114–117 (1972).
3. Geldzahler, R. *et al. Astrophys. J.* **273**, L65–L69 (1983).
4. Lamb, R. C., Fichtel, C. E., Hartman, R. C., Kniffen, D. A. & Thompson, D. J. *Astrophys. J.* **212**, L63–L66 (1977).
5. Vladimirsky, B. M., Neshpor, Y. I., Stepanian, A. A. & Fomin, V. P. *Proc. 14th Int. Cosmic Ray Conf.* **1**, 118–122 (1975).
6. Samorski, M. & Stamm, W. *Astrophys. J. Lett.* **268**, L17–L21 (1983).
7. Hermsen, W. *Proc. 18th ESLAB Symp. X-Ray Astr.* (Scheveningen, in the press).
8. Parsignault, D. R. *et al. Nature* **239**, 123–125 (1972).
9. White, N. E. & Holt, S. S. *Astrophys. J.* **257**, 318–337 (1982).
10. Mason, K. O. *et al. Astrophys. J.* **207**, 78–87 (1976).
11. Bonnet-Bidaud, J. M. & van der Klis, M. *Astr. Astrophys.* **101**, 299–304 (1981).
12. Van der Klis, M. & Bonnet-Bidaud, J. M. *Astr. Astrophys. Suppl. Ser.* **50**, 129–140 (1982).
13. Turner, M. J. L., Smith, A. & Zimmermann, H. U. *Space Sci. Rev.* **30**, 513–524 (1981).
14. Cordova, F., Garmire, G. & Lewin, W. H. G. Final Tech. Rep., NASA NSG **5197**, 1–13 (1978).
15. Milgrom, M. & Pines, D. *Astrophys. J.* **220**, 272–278 (1978).
16. Pringle, J. E. *Nature* **247**, 21–22 (1974).
17. Bignami, G. F., Maraschi, L. & Treves, A. *Astr. Astrophys.* **55**, 155–158 (1977).
18. Davidsen, A. & Ostriker, J. P. *Astrophys. J.* **189**, 331–338 (1974).
19. Pringle, J. E. *A. Rev. Astr. Astrophys.* **19**, 137–162 (1981).
20. Voges, W., Kahabka, P., Ögelman, H., Pietsch, W. & Trümper, J. *Proc. 18th ESLAB Symp. X-ray Astr.* (Scheveningen, in the press).
21. Joss, P. C., Avni, Y. & Rappaport, S. *Astrophys. J.* **221**, 645–651 (1978).
22. White, N. E. *et al. Astrophys. J. Lett.* (in the press).
23. Frank, J. & Sztajno, M. *Astr. Astrophys.* **138**, L15–L16 (1984).
24. Langmeier, A., Sztajno, M. & Trümper, J. *Proc. Conf. X-ray Astr. '84* (Bologna, in the press).
25. Van der Klis, M. & Bonnet-Bidaud, J. M. *Astr. Astrophys.* **95**, L5–L7 (1981).

Transport of venusian rolling 'stones' by wind?

Ronald Greeley & John R. Marshall

Department of Geology, Arizona State University, Tempe, Arizona 85287, USA

Speculation that aeolian processes operate on Venus[1,2] has been confirmed tentatively by analyses of results from Venera spacecraft[3–5]. Here we describe simulations of venusian wind processes, which show that particles are moved by 'rolling' at wind speeds as much as 30% lower than those required for saltation threshold. This mode of wind transport is only observed for sustained periods in water on Earth; thus, there are similarities between aqueous fluid transport on Earth and atmospheric transport on Venus. The formation of small sand ridges and grooves oriented parallel to the wind direction is associated with the rolling of grains in venusian simulations and these structures may be unique aeolian features on Venus.

Because the venusian atmosphere is almost 50 times denser than that of the Earth, wind speeds for particle movement are reduced by about an order of magnitude on Venus compared with Earth. Consequently, the measured near-surface winds of 0.5-1.0 m s^{-1} seem to be well within the range required to transport sand-size particles[6] and aeolian processes may play a significant role in the modification of the surface, both in the formation of landforms, such as dunes, and in the redistribution of sediments. To determine the characteristics of aeolian processes on Venus, a wind tunnel (VWT) capable of simulating the near-surface venusian environment was fabricated. Previous experiments[7,8] have established (1) saltation threshold wind speeds as a function of particle size, (2) the flux of saltating particles, (3) the speed of individual grains, and (4) the nature of small bedforms, such as ripples.

Bagnold[9] has described three modes of aeolian transport on Earth: surface creep, saltation and suspension. Generally, surface creep involves coarse grains ($\leq$4,000 μm), saltation involves coarse silt and sand grains ($\sim$40-4,000 μm) and suspension involves fine particles ($<$40 μm). As the size of grain most easily moved (that is, by weakest winds) is fine-medium sand ($\sim$100 μm) most near-surface windblown particles are moved by saltation. Indeed, on Earth, both surface creep (called 'impact creep' by Sharp[10]) and suspension result primarily from the impact of saltating grains.

Bagnold[9] noted that as wind speed increases over a bed of loose sand grains at rest, the direct pressure of the wind begins to roll some of the grains. At a distance of 30-40 cm downwind from the point where rolling begins, grains increase in speed and begin to saltate, frequently causing a cascading effect in which other grains are set directly into saltation on impact. In our experiments, conducted under terrestrial conditions[11], we find a similar sequence and note that the transition from rolling to fully developed saltation is rather abrupt and the rolling stage is very brief (less than a few seconds), despite careful control of the wind speed. Thus, rolling as a mode of aeolian transport does not appear to be important on Earth in terms of mass transport of material, as it occurs either briefly on attainment of the threshold velocity or intermittently by saltation impact.

In venusian simulations, we ran six sizes of well-sorted particles ranging from fine sand to small pebbles (average diameters are 105, 300, 800, 4,600, 7,800 and 13,000 μm; the three smaller sizes were quartz, the three larger sizes were rounded grains of microcrystalline calcite). For each size, a bed of particles $\sim$1 cm thick was spread evenly over the test plate of the wind tunnel. The tunnel was pressurized to venusian conditions, run briefly at a wind speed above threshold to develop a natural aeolian-textured surface, then stopped[7]. The wind speed was then slowly increased while the test bed was observed through viewing ports and the motion and general behaviour of individual grains were

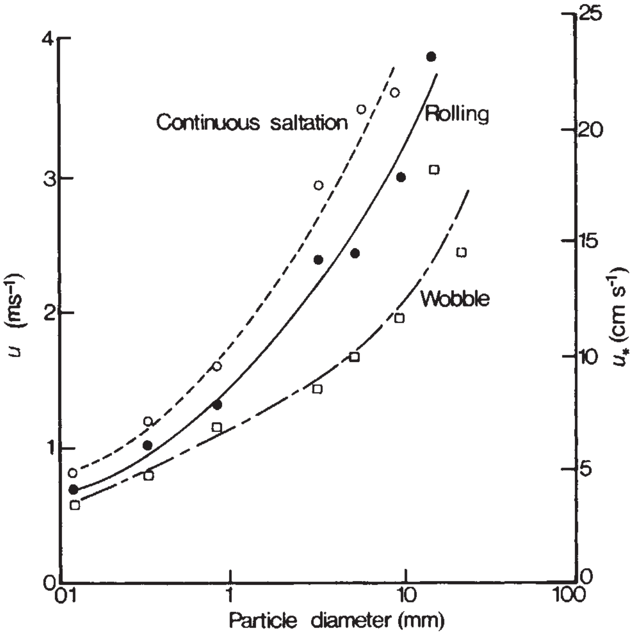

Fig. 1 Wind threshold curves for three types of particle motion in simulations of Venus: u_* is wind friction speed; u_∞ is 'freestream' wind tunnel speed, which can be taken as approximately equivalent to wind speeds measured by the Venera landers.

noted. In some experiments, high-speed (up to 4,500 frames per second) motion pictures were taken through side viewing ports to observe the motion of grains near the bed.

We observed three types of particle motion in these simulations of Venus: wobbling, rolling and fully developed saltation. Previous experiments[7] showed that impact creep also occurs and, although experiments have not been conducted with fine particles, we presume that suspension would also occur on Venus. The threshold wind speeds at which the three types of motion are initiated are shown in Fig. 1 as functions of particle diameter. In wobbling motion, the grains quiver but did not move out of place. At a slightly higher wind speed, the grains began to tumble along the surface in the rolling mode and only a few grains would saltate. Continuous (fully developed) saltation did not occur until markedly high wind speeds were available, especially for large particles. The values shown on Fig. 1 for continuous saltation correspond to the single threshold curves predicted for Venus in previous studies[1,2,6,7]. Thus, when the rolling mode of wind transport is taken into account, wind speeds on Venus for aeolian activity may be 30% less than previous estimates.

The rolling observed in VWT does not lead to a cascading effect, which on Earth ordinarily transforms the surface of the bed rather suddenly into a saltation cloud. Observations that the rolling mode can be maintained in VWT for an indefinite period and that a windspeed can be chosen (for any specified particle size) to maintain rolling are indications that venusian aeolian transport differs significantly from that on Earth. The sub-saltation regime of particle motion in VWT gives rise to a distinctive bedform parallel to the wind direction (Fig. 2). In the rolling mode, the test-bed surface was sculpted into a series of grooves and ridges oriented parallel to the wind for tests with the finest (~105-μm) particles. These features, some of which extended the full length of the test plate, were several millimetres high by several millimetres wide and are remarkably similar in size and form to grooves and ridges produced in mud by unidirectional water currents[12]. Allen suggests[12] that transverse components of flow associated with boundary-layer streaks are involved in eroding the grooves and shaping the bed. Above the saltation threshold, bedforms consist of small ripples and 'microdunes'[8] that are transverse to the wind.

Our results show that the movement of particles in the dense venusian atmosphere resembles that of water-driven particles on Earth. Bagnold[9] compared particle movement in air with particle movement in water on Earth and noted that the fluid/particle density ratio is 1:2,000 in air and 1:2.65 in water; in the dense venusian atmosphere this ratio is approximately 1:40. Thus, aeolian conditions on Venus may share characteristics of both aeolian and aqueous conditions on Earth. For example, we have previously described small dunes (microdunes) that develop in venusian simulations and resemble sand waves formed in water but are absent in air on Earth[8]. In additional venusian simulations, we have observed the development of erosional slip faces on microdunes at high wind velocities (due to reverse flow in the lee eddy), similar to the erosional lee slopes developed in subaqueous bedforms referred to as current ripoles[13]. Furthermore, Gilbert's description[14] of the movement of particles in water is remarkably similar to our own obsevations from venusian simulations. He notes a rolling/saltation mode in which grains roll along the surface and occasionally saltate on short trajectories. Similarly, Abbott and Francis[15] have recognized a distinctive rolling mode for small (centimetre) pebbles in water from high-speed photographs of flume experiments. They note, however, that rolling continues at fluid velocities well above the suspension threshold.

From comparisons with particle transport in water, we infer that the rolling mode is sutained in VWT because of the fluid-particle density ratio in the venusian environment. The fluid is evidently dense enough to generate surface shear for grain motion at velocities well below saltation threshold, similar to water, but, unlike water, is not sufficiently dense to carry the particles aloft in continuous saltation at low velocities.

The rolling mode of wind transport on Venus may be important from several considerations. (1) Frequency of transport: because threshold wind speeds for rolling are significantly lower than for continuous saltation, the occurrence of aeolian processes may be more frequent than is indicated solely on the basis of saltation threshold, despite the relatively gentle winds recorded on Venus. (2) Interpretation of venusian surface: if some bedforms are the consequence of a mode of fluid transport that is unique to the venusian environment, then interpretations of the surface should not rely solely on terrestrial aeolian (or water) analogues. (3) Movement of large particles: particles of 4–5 mm may be easily moved by rolling (Fig. 1), by winds within the range expected on Venus. (4) Flux of windblown material: previous estimates of the amount of material moved by the wind on Venus[16] do not take into account the rolling mode, but are based solely on saltation. Thus, substantial material may be

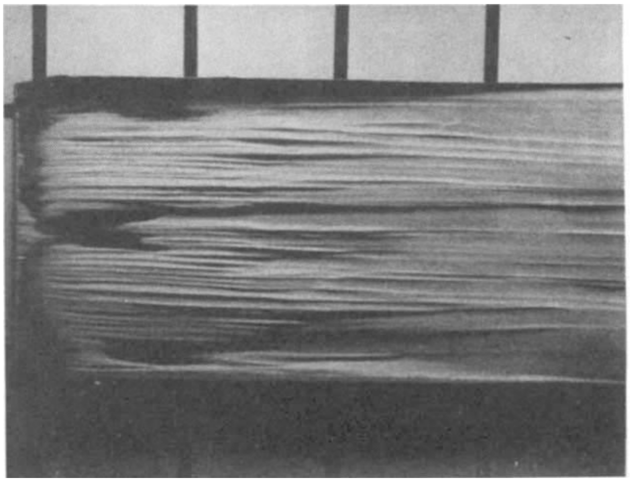

Fig. 2 View of grooves and ridges developed in fine quartz sand (110 μm in diameter) in association with particles rolling along the surface in a simulation of Venus; the windspeed was held below the value required for continuous saltation. Area shown is about 20 by 40 cm; illumination from upper left; wind was blowing from left to right.

moved by surface creep involving rolling (especially for large grains) at relatively low (sub-saltation) wind speeds. However, the total flux may still be far less than that of sediments transported by water on Earth[17]. (5) Small-scale surface features: small features transverse to the wind such as ripples and microdunes did not develop in experiments in which transport occurred solely by rolling. However, grooves and ridges parallel to the wind were formed and thus may be expected on Venus. The length of these features was governed by the size of the wind tunnel and it is possible that on Venus they could extend for tens or even hundreds of metres. Depending on the characteristics of radar imaging systems, such as wavelength, and the geometry of the radar beam, radar signatures from the surface of Venus could be influenced by the presence of these grooves and ridges. In these preliminary results, we note that although there is an association between rolling and longitudinal bedforms, the latter features are not necessarily a function of this mode of transport.

This work was supported by the National Aeronautics and Space Administration Office of Planetary Geology through the NASA-Ames Aeolian Consortium.

Received 1 October; accepted 12 December 1984.

1. Hess, S. L. *J. atmos. Sci.* **32,** 1076–1078 (1975).
2. Sagan, C. *J. atmos. Sci.* **32,** 1079–1083 (1975).
3. Garvin, J. B. *Proc. Lunar planet. Sci.* **12B,** 1493–1505 (1981).
4. Florensky, C. P. *et al. Science* **221,** 57–59 (1983).
5. Basilevsky, A. T. *et al. Bull. geol. Soc. Am.* (in the press).
6. Iversen, J. D. & White, B. R. *Sedimentology* **29,** 381–393 (1982).
7. Greeley, R. *et al. Icarus* **57,** 112–124 (1984).
8. Greeley, R. *et al. Icarus* **60,** 152–160 (1984).
9. Bagnold, R. A. *The Physics of Blown Sand and Desert Dunes,* 1–265 (Methuen, London, 1954).
10. Sharp, R. P. *J. Geol.* **71,** 617–636 (1963).
11. Greeley, R. *et al. Geol. Soc. Am. Spec. Pap.* **186,** 101–121 (1981).
12. Allen, J. R. L. *Sedimentary Structures* Vol. 1, 1–593 (Elsevier, Amsterdam, 1982).
13. Reineck, H. E. & Singh, I. B. *Depositional Sedimentary Environments,* 1–549 (Springer, Berlin, 1980).
14. Gilbert, G. K. *US Geol. Surv. Prof. Pap.* **86,** (1914).
15. Abbott, J. E. & Francis, J. R. D. *Phil. Trans. R. Soc.* **A284,** 225–254 (1977).
16. Greeley, R. *et al. National Aeronatuics and Space Administration TM-82385,* 275–277 (1980).
17. McGill, G. E. *Episodes* **4,** 10–17 (1983).

Neutron generation in lightning bolts

G. N. Shah, H. Razdan, C. L. Bhat* & Q. M. Ali

Bhabha Atomic Research Centre, Nuclear Research Laboratory,
Zakura, Naseem Bagh, Srinagar-19006, Kashmir, India

Intense electrical discharges through polymer fibres have been shown[1] to produce 2.45-MeV neutrons, probably by deuteron–deuteron fusion. Noting broad similarities between discharges in polymer fibres and natural lightning, Libby and Leukens[2] have suggested that neutrons are also generated in lightning flashes, as a result of the fusion of deuterium contained in the atmospheric water vapour; by rescaling the plasma parameters of polymer fibres to those involved in natural lightning, they have predicted a yield of $\sim 10^{15}$ neutrons per lightning flash. An experiment by Fleischer[3], however, using fission track detectors placed near lightning arrestors, has failed to ascertain the neutron production in lightning discharges. Based on the number of background cosmic-ray tracks accumulated in these detectors during seven months of observations, Fleischer estimated an upper limit of 2.5×10^{10} neutrons per lightning stroke. In our experiment, we have attempted to keep the cosmic-ray neutron background at a negligible level by searching for neutrons from individual lightning strokes, for a time-interval comparable with the duration of the lightning stroke. Here we present the first experimental evidence that neutrons are generated in lightning discharges, with 10^7–10^{10} neutrons per stroke. Whether these neutrons are thermonuclear in origin, or are generated by non-thermal processes, remains to be determined.

Neutrons were detected at Gulmarg (altitude 2,743 m, latitude 34.07° N, longitude 74.42° E) by a low-energy cosmic-ray neutron monitor comprising 21 enriched BF_3 counters, each 90 cm long and 3.8 cm in diameter. The counters are arranged in the form of a pile and are placed over 28-cm-thick paraffin wax slabs 8 m above the ground, which helps render the monitor essentially opaque to low-energy background neutrons entering it from below. The counters are also covered from above with 7.5-cm-thick paraffin wax to thermalize 2.45-MeV neutrons and allow their detection with an efficiency of ~3%. The monitor has an effective surface area of $3 \times 10^4\ \text{cm}^2$ and continuously records low-energy cosmic-ray background neutrons with an average rate of 1.8×10^4 neutrons per 30 min. The pressure coefficient for the monitor is −0.66% per mbar, in close agreement with reported values[4,5].

A linear antenna is mounted in the vicinity of the monitor to sense the short-term electric field variation associated with a lightning stroke. The signal, after suitable amplification and amplitude discrimination, activates an interval-counter to count 10-μs pulses from an oscillator, from the instant of the sensing of the electric field to the arrival of the first neutron detected in the pile. The time delay, thus registered in the arrival of the prompt neutron, is used for computing the distance to the lightning stroke, assuming a line-of-sight propagation. This neutron and those detected within the next 320 μs are recorded in four counters, each opened sequentially for an interval of 80 μs and having provision for counting a maximum of 99 neutrons. At the completion of the recording sequence, the time delay and the neutron counts are printed and the system primed for a subsequent lightning event after a dead-time of 400 ms. Note that the total counting time of 320 μs is large compared with the 50-μs duration of a typical lightning stroke and small compared with the average inter-stroke time of 40 ms[6]. The cosmic-ray background is negligible in this time and, thus, it is possible to monitor neutrons from individual lightning strokes with a high signal-to-noise ratio.

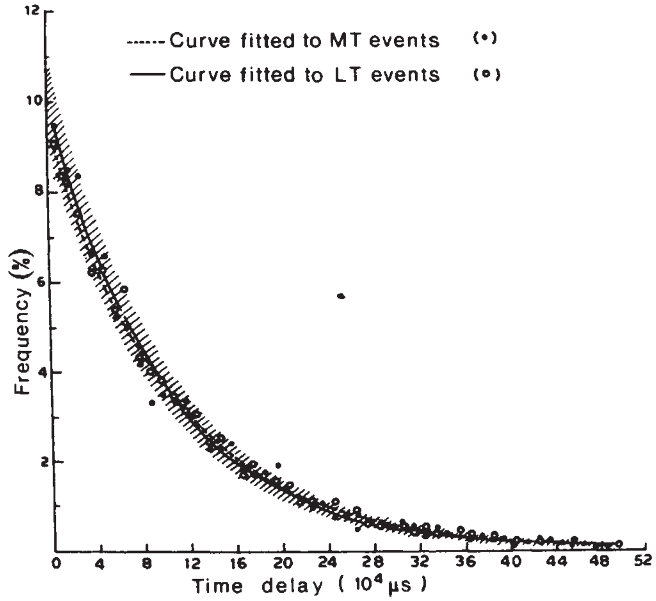

Fig. 1 The time-delay distributions of one-neutron lightning-triggered (LT) and manually-triggered (MT) events. Exponential curves fit both the data sets and produce a mean count rate of 10 neutrons s^{-1}, suggesting that these events are related to the background cosmic rays. The hatched portion represents the error range estimated for the fitted curves.

Between May 1980 and May 1983, the Gulmarg experiment has responded 11,200 times to potential gradient variations from lightning; it has also been activated manually on 8,400 occasions by feeding a pulse generator output to the lightning channel discriminator unit at randomly chosen epochs. Table 1 compares the frequency of the lightning-triggered (LT) events as a function of neutron number recorded per event with the corresponding

---

* Present address: Department of Physics, University of Durham, Durham DH1 3LE, UK.